CFTR Inactivation by Lentiviral Vector-mediated RNA Interference and CRISPR-Cas9 Genome Editing in Human Airway Epithelial Cells

Jessica Bellec[1, 2], Marc Bacchetta[3], Davide Losa[3], Ignacio Anegon[1, 2],
Marc Chanson[3]*, Tuan Huy Nguyen[1, 2]*

[1]INSERM UMR 1064, Centre de Recherche en Transplantation et Immunologie, Nantes, France
[2]CHU Hôtel Dieu, Institut de Transplantation en Urologie et Néphrologie, Nantes, France
[3]Geneva University Hospitals and University of Geneva, Geneva, Switzerland

* Authors contributed equally to this work

Running title: Targeting *CFTR* in polarized airway epithelium

Corresponding author:

Marc Chanson, PhD

Laboratory of Clinical Investigation III

Department of Paediatrics and Department of Cell Physiology & Metabolism

1 rue Michel-Servet

1211 Geneva, Switzerland

Phone: +41 22 37 95 206

Fax: +41 22 37 95 260

marc.chanson@hcuge.ch, marc.chanson@unige.ch

Abstract

Background: Polarized airway epithelial cell cultures modelling *Cystic Fibrosis Transmembrane conductance Regulator* (CFTR) defect are crucial for CF and biomedical research. RNA interference has proven its value to generate knockdown models for various pathologies. More recently, genome editing using CRISPR-Cas9 artificial endonuclease was a valuable addition to the toolbox of gene inactivation.

Methods: Calu-3 cells and primary HAECs were transduced with HIV-1-derived lentiviral vectors (LVV) encoding small hairpin RNA (shRNA) sequence or CRISPR-Cas9 components targeting *CFTR* alongside GFP. After sorting of GFP-positive cells, *CFTR* expression was measured by RT-qPCR and Western blot in polarized or differentiated cells. CFTR channel function was assessed in Ussing chambers. Il-8 secretion, proliferation and cell migration were also studied in transduced cells.

Results: shRNA interference and CRISPR-Cas9 strategies efficiently decreased *CFTR* expression in Calu-3 cells. Strong *CFTR* knockdown was confirmed at the functional level in CRISPR-Cas9-modified cells. *CFTR*-specific shRNA sequences did not reduce gene expression in primary HAECs, whereas CRISPR-Cas9-mediated gene modification activity was correlated with a reduction of transepithelial secretion and response to a CFTR inhibitor. *CFTR* inactivation in the CRISPR-Cas9-modified Calu-3 cells did not affect migration and proliferation but slightly increased basal interleukin-8 secretion.

Conclusion: We generated *CFTR*-inactivated cell lines and demonstrated that CRISPR-Cas9 vectorised in a single LVV efficiently promotes *CFTR* inactivation in primary HAECs. These results provide a new protocol to engineer CF primary epithelia with their isogenic controls and pave the way for manipulation of *CFTR* expression in these cultures.

Keywords: *CFTR*, CRISPR-Cas9, Cystic Fibrosis, lentiviral vector, primary cells, RNA interference

Introduction

Understanding a pathology and its underlying mechanisms benefits from the modulation of gene expression at the cellular or whole organism level. Advances in molecular techniques have allowed the manipulation of gene expression in many cell systems. RNA interference (RNAi) enables fine tuning of gene expression via endogenous long double-stranded DNAs or synthetic micro or small interfering RNAs (miRNA and siRNA). RNAi is a fast, easy and highly efficient means to inactivate target genes but gene repression is transient and restricted to cells suitable to transfection. An alternative approach has been found by means of small hairpin RNAs (shRNA) that can be stably integrated into host cell genome using viral vectors [1]. Lentiviral vectors (LVVs) are particularly well adapted due to their ability to deliver large transgenes into dividing or quiescent cells [2], including primary airway epithelial cells (HAECs) [3–5], and have already been broadly used to induce shRNA-mediated gene knockdown [6]. In parallel, technologies have been developed to directly modify genomic DNA sequences. Artificial endonucleases have been the object of considerable attention due to their ability to create double-strand breaks (DSBs) at a specific locus in genomic DNA (gDNA). The type II clustered regularly interspaced short palindromic repeats (CRISPR)-CRISPR associated (Cas) system from the adaptive immune system of bacteria and archaea provides a novel effective tool for genome editing [7]. Cleavage by the endonuclease Cas9 from *S. pyogenes* is initiated by the recognition of a specific 20-nucleotide DNA sequence and a protospacer adjacent motif (PAM) by a crRNA combined with an activating tracrRNA. A single guide RNA (sgRNA) mimicking this two-RNA structure has been engineered to drive Cas 9-induced DSB [8] facilitating design and vectorization in LVVs [9].

RNAi and genome editing strategies have been successfully used to generate cell and transgenic animal models and for therapeutics purposes [10,11] in various pathologies including cystic fibrosis (CF) [12]. CF is caused by mutations in the *Cystic Fibrosis Transmembrane conductance Regulator* (*CFTR*) gene, which codes for a chloride channel expressed in epithelial barriers[13]. These mutations induce defects in various organ systems but the most common lethal consequence is the development of a chronic lung disease. In the airways, CF is characterized by chronic infection, deleterious inflammation and tissue remodelling. However, how mutations in *CFTR* lead to the development of chronic infection and inflammation remains a matter of debate. Animal models developed in mice, pigs and ferrets [14–18] are valuable for CF research, but they are expensive to handle. Moreover, various aspects of CF show different severities and contribute to the heterogeneous phenotypes between species. Although numerous CF and non-CF cell lines [19] are available to investigate the molecular and cellular defects caused by *CFTR* mutations, bias can originate from culture types and experimental conditions, limiting their interpretation and generating contradictory conclusions.

In this study, we used RNAi and CRISPR-Cas9 genome editing strategies to target *CFTR* gene. Although the inactivation mechanism of both strategies cannot be compared, we sought to evaluate the best approach to induce long-term inactivation in a cellular model capable of polarisation and differentiation. shRNAi and CRISPR-Cas9 strategies were first developed in the Calu-3 cell line, which strongly expresses *CFTR* and form polarized monolayers with intercellular junctions and transepithelial resistances [20]. However, Calu-3 cells cannot resume the morphology of fully-differentiated epithelia. Primary HAECs more closely resemble the native airway epithelium and are capable of differentiation into a pseudo-stratified mucociliated epithelium [21]. Primary cultures can be initiated from CF and non-CF patient airway biopsies. Nonetheless, these cultures remain limited

because of scarce availability of biopsies from CF patients, high variability in terms of genotype, history of infections and treatments, and the lack of isogenic controls. Recently, Ramachandran *et al.* [22] published a protocol to knockdown *CFTR* using siRNA but this requires a maximum seeding density and is not compatible with cell proliferation. Thus, currently, there is no stable *CFTR*-knockdown or knockout model in primary HAECs.

In this study, we have generated two Calu-3 cell lines in which CFTR protein expression is stably reduced either by shRNAi or CRISPR-Cas9 genome editing. Only CRISPR-Cas9-modified cells reproduced the characteristic CFTR-mediated current defect and showed increased release of the pro-inflammatory mediator interleukin (IL)-8. Optimized molecular tools and protocols were also applied to primary HAECs. Transduction with HIV-1 LVV expressing CRISPR-Cas9 system efficiently knocked-down *CFTR* gene. Our work has led to the generation of *CFTR*-inactivated cell lines and new vectors demonstrating the great potential of CRISPR-Cas9 system for CF disease modelling in differentiated primary HAECs.

Materials and Methods

Cell culture

Human airway epithelial Calu-3 cells (HTB-55™) were purchased from the American Type Culture Collection (ATCC, Manassas, VA) and maintained in Minimum Essential Medium (MEM) supplemented with 10% Foetal Bovine Serum (FBS), 1% non-essential amino acids, 1% sodium pyruvate and 1% penicillin/streptomycin. All reagents except FBS were purchased from Life Technologies (Saint-Aubin, France). Well-polarized monolayers of Calu-3 cells were obtained by seeding $1\text{-}1.5\times10^5$ cells onto 0.33cm² porous (0.4µm) Transwell polyester inserts (Transwell 3470, Corning Life Sciences, Hazebrouck, France) and cultured for 14-20 days under submerged conditions.

Primary HAECs were purchased from Epithelix (Plan-Les-Ouates, Switzerland) and maintained according to manufacturer's instructions. To obtain well-differentiated primary epithelia, primary HAECs were seeded at 2.5×10^5 cells onto 0.33cm² porous (0.4µm) Transwell polyester inserts and left to proliferate in CNT17 medium (CellnTec, Bern, Switzerland). Differentiation was induced by culture at the air-liquid interface (ALI) for at least 30 days [23].

DNA constructs

siRNA sequences targeting CFTR mRNA were designed by using the Genelink software (Hawthorne, NY, USA). This led to 460 possible sequence candidates, the specificity of which was verified with Nucleotide BLAST. Out of the 68 sequences selected, four were considered because they did not show any single-nucleotide polymorphisms or insertion/deletion events. Two more sequences were added (Supplementary Figure 1A) and their efficiency was evaluated in two *CFTR*-expressing cell lines. The results of this screen are shown in Supplementary Figures 1B and 1C. Three sequences were retained to design shRNAs. Thus, three CFTR specific siRNAs (sequence 1 5'-TTGGATGACCTTCTGCCTCTTAC-3', sequence 2: 5'-AACAACAGGAGAAGGAGAAGGAA-3' and sequence 3: 5'-GATAGAAAGAGGACAGTTGTTGG-3') and one non-specific siRNA (Alter: 5'-GATAGAAAGGATTGACAGTGGTG-3') were embedded in the following structure, 5'-CGCGTCCCC-sense siRNA-TCAAGAG-anti-sense siRNA-TTTTTGGAAAT-3', to form shRNA sequences. shRNA oligos were then cloned into pLVTHM (Addgene 12247, kind gift from D. Trono, EPFL, Switzerland) LVV backbone in *MluI-ClaI* restriction sites to obtain sh1, sh2 and shAlter DNA constructs.

Cas9-HA-GFP sequence from plasmid pMJ920 (Addgene 42234) was cloned downstream the spleen focus-forming virus (SFFV) promoter in the HIV-1-derived lentiviral vector backbone RRLSIN-cPPT-SFFV-GFP-WPRE (kindly provided by Els Verhoyen, INSERM U1111, France) to produce the control plasmid (CTL). Two N19NGG sequences targeting CFTR exon 2 (TSJB1: 5'-CACCGAAAGGATACAGACAGCGCC-3' and TSJB2: 5'-CACCGGTATATGTCTGACAATTCC-3') were cloned into plasmid pX330-U6-Chimeric_BB-CBh-hSpCas9 (Addgene 42230) in *BbsI* cloning sites. Each pU6-single-guideRNA (sgRNA) expression cassette containing a targeting sequence corresponding to nucleotides 117 504 274 to 117 504 296 (TSJB1) and 117 504 292 to 117 504 314 (TSJB2) in *CFTR* exon 2 was PCR-amplified and introduced into CTL plasmid to produce TSJB1 and TSJB2 plasmids.

HIV-1-derived lentiviral vector production and cell transduction

HIV-1-derived LVVs were produced using the triple transfection method with calcium phosphate [24]. Briefly, HEK293T cells were transfected with the LVV plasmid of interest, the packaging plasmid psPAX2 (Addgene 12260) and the vesicular stomatitis virus G (VSV-G) envelop protein coding plasmid pMD2.G (Addgene 12259). Media was replaced 18 hours post-transfection. Media was supplemented with 10mM sodium butyrate for the production of CRISPR LVVs. Supernatant containing lentiviral vector particles was harvested 24 hours later. Viral stocks were concentrated at 10 000 rpm and 4°C for 18-20 hours, resuspended in advanced Dulbecco's Modified Eagle Medium (DMEM, Life Technologies) and stored at -80°C. LVV titre was determined by flow cytometry following transduction of HeLa cells with a dose range of concentrated vector. Titre was calculated as follows: ((% of GFP positive cells/100) × number of cells at transduction × dilution factor)/volume added, and expressed as [HeLa]transducing units (TU)/mL. Titres ranged from 10^7-10^9 [HeLa]TU/mL depending on the transgene of interest.

Flow cytometry Analysis and Cell Sorting (FACS)

Flow cytometric analysis of cells transduced with HIV-1-derived LVVs was performed using a FACS CantoII and the BDFacsDiva software (BD Biosciences, Le pont de Claix, France). Percentages of GFP positive cells were determined using FlowJo software.

Sorting of GFP positive cells was performed using a FACS Aria (BD Biosciences) at the flow cytometry core facility of the Medical Faculty (Geneva, Switzerland).

T7EI mismatch detection assay

Genomic DNA (gDNA) was extracted using a phenol-chloroform protocol and quantified using the NanoDrop2000 spectrophotometer (Thermo Fisher Scientific, Illkirch, France). A260/A280 and A260/A230 ratios accounted for sample purity.

Gene modification activity of sgRNA sequences at the target locus of *CFTR* exon 2 and at the four most probable off-target sites (http://crispr.mit.edu [25]) was quantified using the T7EI mismatch detection assay. DNA sequence of interest was PCR-amplified using Taq Platinum HiFi polymerase (Invitrogen™, Life Technologies), forward primer 5'-TGTAGCCTGTAAGAGATGAAGC-3' and reverse primer 5'-CAATCCTCTCATCTTGGCCTC-3'. The 451bp PCR product was then denatured and slowly re-annealed (95°C, 2min ; 95°C to 85°C, -2°C/sec ; 85°C to 25°C, -1°C/sec) to produce homoduplex/heteroduplex mix. This was then digested by the T7E1 restriction enzyme (3 units) at 37°C for 30 minutes. Digestion products were separated by capillary gel electrophoresis using Caliper (Perkin Elmer, Waltham, MA) and their relative amounts was calculated using the LabChip GX Touch data analysis software (Perkin Elmer).

Reverse Transcription quantitative Polymerase Chain Reaction

Total RNA was extracted using the NucleoSpin® RNA II kit (Macherey Nagel, Hoerdt, France) and quantified using the NanoDrop2000 spectrophotometer (Thermo Fisher Scientific). A260/A280 and A260/A230 ratios accounted for sample purity. Reverse transcription was performed using the Quantitect reverse-transcriptase kit (Qiagen, Courtaboeuf, France) and 200ng RNA following manufacturer's protocol. PCR were performed by the genomic core facility of the Medical Faculty (Geneva, Switzerland) using TaqMan gene expression assays and TaqMan Fast master mix (Applied Biosystems, Life Technologies) according to the manufacturer's instructions. Reactions were performed in triplicate and the relative abundance of CFTR mRNA was calculated using the $\Delta\Delta$ cycle threshold method relative to glyceraldehyde-3-phosphate dehydrogenase (GAPDH) mRNA abundance.

Western blotting

Proteins were incubated in a solubilisation buffer (65mM Tris, 150mM NaCl, Nonidet-P40 1%, protease inhibitor mix 1X (Roche)) for 30 minutes at 4°C. Samples were then centrifuged at 10 000×g and 4°C for 15 minutes and supernatant was harvested and stored at -20°C until use. Proteins were quantified by a bicinchoninic acid (BCA) assay (Pierce, Thermo Fisher Scientific). Equal amounts of total protein were separated on a sodium dodecyl sulphate polyacrylamide gel electrophoresis (SDS-PAGE) and transferred on a polyvinylidene fluoride (PVDF) or a nitrocellulose membrane using the semi-dry transfer technic. Membranes were blocked in TBS-T buffer (20mM Tris, 140mM NaCl, Tween-20 0.1%) containing 5% defatted milk for a minimum of 1 hour at room temperature (RT) under agitation. Membrane was first incubated with mouse monoclonal anti-human CFTR antibody (C-Terminus clone 24.1, MAB25031, R&D Systems, Lille, France) or mouse monoclonal anti-GAPDH antibody (clone 6C5, MAB374, Millipore, Guyancourt, France) diluted 1:1000 and 1:2000, respectively, in TBS-T buffer containing 1% defatted milk. Membranes were then blotted with polyclonal goat anti-mouse Horse Raddish Peroxidase (HRP)-conjugated antibody (Jackson ImmunoResearch Laboratories, West Grove, PA) and revealed using SuperSignal West Pico kit (Pierce, Thermo Fisher Scientific). Band intensities were quantified using ImageJ software. CFTR expression was normalized to GAPDH.

Electrophysiological studies

CFTR channel activity was assessed by measurement of transepithelial short-circuit currents (Isc) in Ussing chamber device (Physiologic Instruments, San Diego, CA). Basal chamber was filled with a Krebs buffer containing 134mM NaCl, 4.8mM KCl, 1.2mM KH_2PO_4, 1.2mM $MgSO_4$-$7H_2O$, 5mM $NaHCO_3$, 2.5mM $CaCl_2$, 10mM Hepes and 1mM glucose (pH 7.4). Apical chamber was filled with a Krebs buffer containing 119mM Na gluconate, 15mM NaCl, 4.8mM K gluconate, 1.2mM KH_2PO_4, 1.2mM $MgSO_4$-$7H_2O$, 5mM $NaHCO_3$, 2.5mM $CaCl_2$, 10mM Hepes and 1mM glucose (pH 7.4). The transepithelial potential difference was voltage-clamped at zero and the resulting Isc was recorded using a VCC MC6 amplifier (Physiological Instruments). Data were acquired using the interface DI-720 (DataQ Instruments) and Acquire & Analyze software 2.3 (Physiological Instruments). Fluid currents while using different basal and apical medium were not cancelled. For some experiments, cells were pre-treated with 10 μM indomethacin for 1 hour to decrease basal CFTR activity and improve stability of the recordings. Epithelial sodium channel (ENaC)-mediated currents were blocked by the addition of amiloride (100μM final concentration) in the apical chamber. CFTR-mediated currents were stimulated

by the addition isoproterenol (100µM final concentration) in the basal chamber and finally inhibited by the addition of the specific blocker I-172 (20µM final concentration) in the apical chamber.

Migration and proliferation assay

To assess migration and proliferation properties of shRNA- or CRISPR-modified Calu-3 cells, untransduced, shAlter, sh1+sh2, CTL and TSJB1 cells (5×10^4) were seeded in silicone culture-inserts (IB-80209, Ibidi, Biovalley, Marne-la-Vallée, France) and cultured until confluence at which point the chambers were removed (t=0h). Gap closure was monitored 15 hours later (t=15h). Pictures were taken at t=0h and t=15h using the EVOS FL microscope (AMG, Bothell, WA) and the entire gap surface was reconstructed using Photoshop software. The gap area was measured as a pixel number using ImageJ software.

To quantify the number of proliferating cells, inserts were fixed in 4% paraformaldehyde for 15min and then processed in the following solutions: PBS-Triton 0.1% for 10min, NH_4Cl 0.5M for 15min and PBS-BSA 2% for 15min. Calu-3 cells were then incubated with the monoclonal anti-Ki-67 antibody (1:100 dilution, mib1, DAKO, Les Ulis, France) followed by a goat anti-mouse Alexa 568 antibody (1:1500, Jackson ImmunoResearch Laboratories). DAPI was used to stain nuclei. Ki-67 and DAPI-positive cells were counted using ImageJ software.

IL-8 secretion

Basal secretion of the pro-inflammatory chemokine interleukin (IL)-8 was measured in Calu-3 cells 11 days post-seeding and in untransduced and transduced HAECs isolated from one patient and differentiated for 31-36 days at ALI. Apical and basolateral media were collected 24h after the last media change and IL-8 secretion was determined using Human IL-8 ELISA Ready-SET-Go! (2nd generation) kit (Ref 88-8086-22, Affymetrix eBioscience, Paris, France), according to the manufacturer's protocol. Samples were diluted 1:200 and assayed in triplicate. Total proteins were extracted and quantified as described above and were similar in the different Calu-3 cell (2.4 ±0.08 mg in untransduced cells, 2.3±0.04 mg in cells transduced with CTL LVV, 2.3±0.05 mg in cells transduced with TSJB1 LVV) or HAEC samples (0.08mg in untransduced cells, 0.06mg in cells transduced with CTL LVV and 0.09mg in cells transduced with TSJB1 LVV). IL-8 secretion was normalized to the total amount of proteins.

Statistical analysis

Data are presented as means ± standard error of the mean (SEM). Statistical significance was calculated using GraphPad Prism software with a p value <0.05 considered as significant. Cell populations were compared using the non-parametric Kruskal-Wallis test with the Dunn's multiple comparisons test correction or a Mann-Whitney test. * $p<0.05$, ** $p<0.01$, *** $p<0.001$, **** $p<0.0001$

Results

Transduction with HIV-derived lentiviral vector allowed stable expression of shRNA constructs and active CRISPR-Cas9 system in Calu-3 and primary human airway epithelial cells

To stably silence *CFTR* gene in Calu-3 cells and primary HAECs, we cloned three shRNA sequences against CFTR mRNA selected among six sequences and a non-specific shRNA sequence (shCFTR and shAlter respectively) in a HIV-1-derived LVV backbone also expressing the GFP reporter gene (Supplementary figure 2A). In parallel, we also designed and cloned two single sgRNA targeting *CFTR* exon 2 (TSJB1 and TSJB2), alongside the Cas9-HA-GFP expression cassette in a HIV-1-derived LVV backbone. The construct lacking a sgRNA sequence was used to generate a control cell line (CTL Calu-3 cells, Supplementary figure 2A). shRNA and CRISPR-Cas9 LVVs efficiently transduced both Calu-3 cells and primary HAECs as shown by FACS analysis of GFP expression (46 ±4% in Calu-3 cells with multiplicity of infection (MOI) of 2, 65 ±2% in Calu-3 cells with an MOI of 10, and 68 ±4% in HAECS with a MOI of 10, Supplementary figure 2B). The optimal MOI was determined using dose ranges of LVVs in Calu-3 cells. MOI 10 was the optimal dose regarding transduction efficiency and cytotoxicity using shRNA LVVs (data not shown). The three shCFTR sequences were assessed for their ability to inhibit *CFTR* gene expression. shCFTR and shAlter Calu-3 cell lines were generated by transduction or co-transduction with LVVs followed by FACS sorting of GFP positive cells. *CFTR* silencing was assessed by RT-qPCR and western blot. The combination of shCFTR sequence 1 and shCFTR sequence 2 (sh1+sh2 in Calu-3 cells) induced the more effective knockdown activity (data not shown). Calu-3 cells were also transduced with a dose range of CRISPR-Cas9 LVVs. A week post-transduction, GFP fluorescence and CRISPR-Cas9 activity were measured by FACS and using the T7EI mismatch detection assay, respectively. MOI 2 was the optimal dose as shown in Figure 1A. Indeed, despite the fact that the transduction efficiency was slightly lower at MOI 2, the cleaving activity did not increase with the LVV dose at transduction. Target sequence TSJB1 gave both higher levels of transduction and CRISPR-Cas9 activity (Figure 1A) which was sustained overtime in the resultant cell line (TSJB1 Calu-3 cells, Figure 1B). Off-target effects are the major concern when using artificial endonucleases for genome editing. However, non-specific cleaving activity was not detected in CTL or TSJB1 Calu-3 cell lines in the four most probable off-target sites (Figure 1C).

In view of these observations, primary HAECs were transduced with shRNA LVVs (shAlter, sh1 and sh2) at MOI 10. Two doses were tested for CRISPR LVVs (CTL and TSJB1). GFP positive cells were FACS sorted a week post-transduction to measure CRISPR-Cas9 activity by the T7EI mismatch detection assay. Modification activity was about two-fold higher with a MOI of 10 compared to a MOI of 2 (41% and 48% compared to 18% and 29% respectively, Figure 1D). Thus, this dose was used for consequent experiments in primary HAECs.

shRNA interference and CRISPR-Cas9 genome editing induced stable CFTR inhibition in Calu-3 cells

To quantify the consequences of shRNA interference and CRISPR-Cas9 genome editing in our Calu-3 cells lines, untransduced (UTC), shAlter, sh1+sh2, CTL and TSJB1 Calu-3 cells were cultured on semi-permeable supports under submerged conditions for 14-20 days and *CFTR* inactivation was assessed by RT-qPCR and western blot.

CFTR mRNA in sh1+sh2 Calu-3 cells (0.3 fold change ±0.04, n=6) was reduced by 63% (p=0.0006) compared to shAlter Calu-3 cells (0.8 fold change ±0.07, n=7, Figure 2A). Western blot confirmed this inactivation with a decrease of 77% (p=0.002) of the protein content in sh1+sh2 Calu-3 cells (0.3 fold change ±0.09, n=6) as compared to shAlter Calu-3 cells (1.4 fold change ±0.2 n=5, Figure 2C). No statistical difference was observed in CFTR mRNA and protein contents between UTC and shAlter Calu-3 cell lines.

No difference in CFTR mRNA content was observed between CTL and TSJB1 Calu-3 cells (1.2 fold change ±0.07 in TSJB1 cells compared to 1.3 fold change ±0.1 in CTL cells, Figure 2B) indicating that CRISPR-Cas9 activity confirmed in TSJB1 Calu-3 cells (Figure 1B) did not induced mutations that altered expression of CFTR mRNA sequences that can be detected by RT-qPCR. However, the decrease of CFTR protein expression was confirmed by Western blot (-70%, p<0.0001) in TSJB1 Calu-3 cells (0.3 fold change ±0.05, n=8) compared CTL Calu-3 cells (n=8, Figure 2D). No difference was observed in CFTR protein content between UTC and CTL Calu-3 cell lines.

In summary, these results indicate that shRNA expression and CRISPR-Cas9 activity efficiently induced strong and stable *CFTR* inactivation in Calu-3 cells.

CRISPR-Cas9 system strongly impaired CFTR function at the electrophysiological level in Calu-3 cells and primary HAECs

CF phenotype is characterized by the alteration of transepithelial currents particularly by a poor or absence of chloride fluxes through CFTR channels [26]. We therefore determine whether *CFTR* inactivation at the post-transcriptional level correlates with the defect of CFTR-mediated currents in modified Calu-3 cells. UTC, shAlter, sh1+sh2, CTL and TSJB1 Calu-3 cells were cultured on semi-permeable supports under submerged conditions for 14-20 days and short-circuit currents (Isc) were studied in Ussing chamber device. After stabilization of the polarized monolayers (Isc_{basal}), CFTR channels were stimulated with isoproterenol, a β2 adrenergic receptor agonist which activates protein kinase A (PKA) via the rise of intracellular cAMP concentration ($Isc_{act. CFTR}$). CFTR-mediated currents were finally inhibited by the specific blocker I-172 ($Isc_{inh. CFTR}$). Representative recordings of transepithelial currents in CRISPR-Cas9 Calu-3 cells are shown in Figure 3A. Isoproterenol induced large outward currents from a lower basal Isc that could be inhibited by I-172, indicating that currents were carried by CFTR (Figure 3A). Isc changes following activation and inhibition of CFTR channels were significantly lower in TSJB1 Calu-3 cells (+8.1 ±2.2 µa.cm² and -8.3 ±2.1 µa.cm², n=7) compared to CTL Calu-3 cells (+44.6±12.7 µa.cm² and -43.3±11.6 µa.cm², n=8, Figure 3C) but not in sh1+sh2 Calu-3 cells (+10.3±2.6 µa.cm² and ±2.7 - 14.4µa.cm², n=10) compared to shAlter Calu-3 cells (+11±2.7 µa.cm² and -17.7±2.4 µa.cm², n=10, Figure 3C). Figure 3D and 3E show the fold changes of CFTR-mediated currents following inhibition relative to UTC cells. Only Calu-3 cells modified with CRISPR-Cas9 system showed a strong 79% *CFTR* knockdown at the electrophysiological level (0.36 ±0.05 fold change in TSJB1 cells, n=7, compared to 1.74 ±0.2 fold change in CTL cells, n=8, p=0.0002). These results demonstrate that *CFTR* inactivation by shRNA interference does not support a loss of function characteristic of CF phenotype compared to CRISPR-Cas9 modified Calu-3 cells. These cell lines therefore may represent a good model for CF.

shRNA interference and CRISPR-Cas9 genome editing strategies were evaluated in primary HAECs, as described in Supplementary figure 3. Cells were cultured at the ALI for 30-40 days and assayed for CFTR

expression as well as for Iscs. Western blot quantifications of the effect of each strategy (Figures 4A and 4B) on CFTR expression showed that shCFTR expression did not affect CFTR protein content whereas CFTR protein expression was reduced by 37% in TSJB1 HAECs (0.63 ±0.09 fold change, n=3) compared to UTC HAECs (1.00 ±0.23 fold change, n=3). For Ussing chamber recordings, epithelia were stimulated as described for Calu-3 cells except that ENaC channels were inhibited by the addition of amiloride before CFTR activation by isoproterenol (Supplementary Figure 4). Transepithelial resistances were measured in all epithelia and confirmed primary HAECs polarization (Figure 4C and 4D). Transduction with sh1 and sh2 LVVs did not knockdown *CFTR* at the electrophysiological level compared to shAlter cells (n=4, Figure 4E). In contrast, expression of CRISPR-Cas9 system induced an 87% decrease (p=0.0571) of transepithelial current variations following CFTR channel inhibition by I-172 in TSJB1 epithelia (n=3) compared to UTC ones (n=4), and a 79% decrease (p=0.0012) of transepithelial current variations following CFTR channel inhibition by I-172 in TSJB1 epithelia (n=6) compared to CTL ones (n=7, Figure 4F). These results confirm that our CRISPR-Cas9 LVV construct can efficiently target *CFTR* expression in primary HAECs.

Combination of shRNA and CRISPR-Cas9 strategies did not further improve CFTR inactivation

shRNA induced *CFTR* knockdown at the protein level but the effect on transepithelial currents was not strong enough to mirror electrophysiological CF defect. Genome editing by CRISPR-Cas9 system significantly reduced but did not abrogate CFTR-mediated currents. We therefore investigated whether the combination of both strategies would lead to complete *CFTR* inactivation. CTL and TSJB1 Calu-3 cells were transduced with shAlter and sh1+sh2 LVVs at MOI 10 respectively. CRISPR-Cas9 cleaving activity did not affect CFTR mRNA (Figure 2B). Following transduction of TSJB1 Calu-3 cells with sh1 and sh2 LVVs, mRNA levels were reduced by 50% (p=0.0143) as shown in Figure 5A (0. ±0.03 6 fold change in TSJB1/sh1+sh2 cells, n=4, compared to 1.2 ±0.05 fold change in CTL/shAlter cells, n=4). However, shRNA interference did not further reduce CFTR protein expression (0.4 ±0.08 fold change in TSJB1/sh1+sh2 cells, n=4, compared to 1.2 ±0.7 fold change in CTL/shAlter cells, n=4, -67%, Figure 5B) and CFTR-mediated transepithelial currents (0.6 ±0.12 fold change in TSJB1/sh1+sh2, n=5, compared to 3.2 ±0.6 fold change in CTL/shAlter cells, n=5, -81%, Figure 5D and 5E) in the TSJB1 Calu-3 cells. The double-knockdown strategy therefore is not the best approach to induce long-term *CFTR* inactivation.

CRISPR-Cas9 CFTR inactivation enhanced interleukin-8 release by Calu-3 cells

To examine the effect of *CFTR* inactivation on Calu-3 cell phenotype, we monitored cell migration and proliferation as well as release of the pro-inflammatory chemokine IL-8. Gap healing experiments were performed on CTL and TSJB1 Calu-3 cells. As shown in Figure 6A, no difference in the gap healing rate measured after 15 hours was observed between CTL (0.7 ±0.04 initial surface repaired, n=10) and TSJB1 Calu-3 cells (0.7 ±0.03 surface repaired, n=11). Cell proliferation was also determined at 15 hours by immunodetection of the nuclear marker Ki-67. Ki-67 proliferation index was similar in both cell lines (47 ±0.02 % Ki-67 positive cells in CTL cells compared to 46 ±0.02 % in TSJB1 cells, n=25, Figure 6B). Together these results indicate that *CFTR* inactivation does not affect cell proliferation and migration in *CFTR* knocked-down Calu-3 cells. We next measured the release

of IL-8 by CTL and TSJB1 Calu-3 cells polarized on Transwell inserts. IL-8 release was measured in apical (Figure 6C) and basolateral (Figure 6D) media and fold change of IL-8 secretion from the CRISPR-Cas9 cells was expressed compared to UTC cells. As shown, transduction of Calu-3 cells enhanced basal level of IL-8 release as compared to UTC cells, although this was not significant. Comparison between CTL and TSJB1 cells revealed that only apical IL-8 secretion was increased in TSJB1 cells (+28%, p=0.0087, n=6). No difference was observed in the basolateral release of IL-8 between CTL and TSJB1 transduced cells. In summary, these results indicate that *CFTR* silencing in Calu-3 cells enhanced IL-8 secretion but did not affect their migratory and proliferating properties.

IL-8 secretion by UTC HAECs and HAECs transduced either with CTL or TSJB1 LVVs was measured in triplicate in apical (Figure 6E) and basolateral (Figure 6F) media. Although a tendency to enhanced basal production of IL-8 was observed in TSJB1 HAECs, the difference did not reach significance.

Discussion

In the present study, we evaluated the efficiency of lentiviral-mediated shRNA and CRISPR-Cas9 strategies to inactivate the expression of *CFTR* gene and impact the phenotype of polarized HAECs. We report high transduction efficiency with both LVVs in the Calu-3 cell line and in primary HAECs. Expression of shRNA sequences and CRISPR-Cas9 system was associated with decreased expression of *CFTR*. However, only the CRISPR-Cas9 strategy reduced CFTR activity in terms of ion transport in polarized epithelia. In addition, CFTR knocked-down Calu-3 cells with the CRISPR-Cas9 strategy retained normal migration and proliferation profiles but showed enhanced apical release of the pro-inflammatory chemokine IL-8. To our knowledge, this is the first report using the CRISPR-Cas9 molecular tool to generate CF-like airway epithelial cell models.

HIV1-derived LVVs were used to mediate shRNA interference and genome editing using CRISPR-Cas9 system to stably knockdown *CFTR*. Indeed, viral gene transfer is more efficient than non-viral delivery methods, particularly in primary cells. LVV was chosen in preference to adenovirus or adeno-associated virus (AAV), for its ability to transduced both quiescent and non-quiescent cells, to integrate a transgene within the host genome, and its large encapsidation capacity [27]. HIV-derived LVVs were pseudotyped with VSV-G envelop for its broad tropism and its stability, allowing production of high titre vector stocks. Consistently high transduction efficiencies were obtained in both Calu-3 cells and primary HAECs as measured by GFP expression. This was dose- and vector-dependent and in agreement with previous studies using HIV-derived LVVs in AECs [3,4,28]. Particularly Borok *et al.* obtained 30% and 80% of GFP-positive cells following transduction of rat AECs with MOIs of 1.6 and 12.8 respectively. Although similar levels of transfection can be obtained with small interfering oligonucleotides [22,29], this does not allow stable integration and expression. Expression of the GFP reporter gene encoded in our shRNA and CRISPR-Cas9 plasmids allowed real-time monitoring of cell lines or cultures purity overtime and over cytotoxicity of the integrated transgenes.

Vectors and transduction strategy were optimized in Calu-3 cells. This cell line is a good model to study delivery in HAECs [30,31] and is broadly used to study CFTR ion channel properties in a human airway epithelial cell line [20]. The LVV-mediated shRNA strategy efficiently knocked-down CFTR protein expression but moderately affected CFTR function at the electrophysiological level. Two *CFTR* knockdown Calu-3 cell lines have already been developed. Palmer *et al.* obtained strong CFTR mRNA and protein expression inhibition associated with 8-cpt-cAMP-mediated secretion decrease (>90%) following transfection with a sleeping-beauty transposon and puromycin selection [32]. Mac Vinish *et al.* obtained less than 5% wild-type CFTR protein content associated with a 75% decreased of cAMP-dependant chloride secretion following stable transfection with siRNA oligonucleotides and clonal selection [33]. More recently, Ramachandran *et al.* used a reverse transfection protocol with siRNA and obtained high *CFTR* knockdown [22]. Protein levels were similar to those observed in this study but inactivation at the functional level was stronger. Several groups have used LVV-mediated shRNA interference in Calu-3 cells [34–37]. Knockdown efficiency is highly target- and protocol-dependent (especially siRNA sequence). Modest *CFTR* knockdown in our Calu-3 cell line may be due to less potent shRNA sequences, although we have selected the two more efficient ones out of six that were initially tested, or to steric hindrance in the targeted region of mRNA. It is also possible that high expression of shRNA constructs saturates cellular RNAi machinery and reduces knockdown efficiency as reported by Grimm [38]. Overexpression of AGO2 and exportin-5 proteins have been shown to enhance silencing efficiency and reduce cytotoxicity [38,39] and might improve

CFTR inactivation. Finally, our sh1+sh2 cell line is not a clonal population. Generation of clonal sh1+sh2 Calu-3 cell line could have greatly improved knockdown efficiency, but our aim was to test our shRNA tool in view of its potential application in primary cultures of airway epithelial cells.

Gene silencing by RNAi is usually not complete. By targeting mRNAs, off-target effects are very likely but these are not easily identifiable. Artificial endonucleases directly target gDNA and are able to introduce silencing mutations within the cell genome, thus eliminating interference with the cellular machinery. Recently, the CRISPR-Cas9 system have been developed and proposed a cost and time-effective alternative to zinc finger and transcription activator-like effector (TALE) nucleases. Off-target modification activity was not detected in the top four off-target sites confirming that CRISPR-Cas9-mediated knockdown is *CFTR*-specific. Furthermore, we did not detect cell toxicity albeit constitutive expression of Cas9 and sgRNA, as shown by GFP cell expression. Using this strategy, we observed strong functional inactivation of the CFTR channel similar to the decrease observed in the protein content. Thus, shRNAs were efficient to knockdown CFTR expression but the remaining CFTR channels were fully functional, indicating that 20% of the total CFTR protein was sufficient to carry out virtually 80% of I-172-inhibitable CFTR currents. In contrast, the CRISP-Cas9 likely introduced a variety of mutations into the *CFTR* sequence, reducing the amount of proteins that could be detected by Western blot by our C-terminal targeted antibody. We assume that most mutant CFTR channels detected by our antibody are dysfunctional, explaining the reduced Isc. The type of mutations introduced by the CRISPR/Cas9 system or whether silencing mutations were induced on both alleles is not known. Therefore, the TSJB1 cell line probably contains cells with one normal *CFTR* allele leading to a residual channel function sufficient to maintain residual CFTR-mediated currents, although additional sequencing of the targeted exon would be necessary to confirm this hypothesis. To circumvent this limitation, we tested a dual strategy combining shRNA expression in CRISPR-Cas9-modified Calu-3 cells. However, *CFTR* knockdown was not improved and transepithelial currents were abnormally enhanced in cells transduced with control vectors. Despite a residual CFTR function, the CRISPR-Cas9 *CFTR* knocked-down cell line represents an interesting model of CF. Indeed, CF-causing mutations from classes III to VI affect the number or the stability of normal proteins at the apical membrane of epithelial cells or the channel functionality [13]. These mutations are responsible for milder forms of CF in patients and are associated with residual CFTR function. F508del, the most common severe CF-causing mutation, is associated with protein folding defect, enhanced degradation, and reduced trafficking and stability. Although the paradigm is an absence of CFTR protein at the apical membrane, few reports showed F508del-CFTR localization at the apical membrane [40–42] and residual chloride secretion function [43–45].

Although CFTR is a chloride channel, *CFTR* mutations have been associated with several other phenotypes including altered cell proliferation and migration during epithelial wound repair [46–48]. However, migration and proliferation were not impaired in our CRISPR-Cas9 *CFTR* knocked-down Calu-3 cell line compared to control cells. CF lung disease is also characterized by deleterious inflammation and excessive secretion of inflammatory cytokines. Interestingly, we observed a significant increase of apical IL-8 release by the CRISPR-Cas9 *CFTR* knocked-down Calu-3 cells in absence of bacterial stimulation. These results are in accordance with previous reports of intrinsic pro-inflammatory state associated with mutated CFTR [49–52]. Non-significant difference of IL-8 secretion at the basolateral side of TSJB1 Calu-3 cells might explain the contradictory results obtained when IL-8 secretion is measured in primary HAECs cultured at the air-liquid interface. Thus, our

cell lines may represent interesting new *in vitro* models of polarized airway epithelial cells to investigate further the links between CFTR and signalling pathways leading to a pro-inflammatory phenotype.

High transduction efficiency and use of GFP reporter gene are particularly useful to rapidly sort high amounts of transduced cells that cannot be cultured for extended periods of time without losing their ability to polarize and differentiate. CRISPR-Cas9 system has been developed very recently and only few references report LVV-mediated knockdown using this artificial endonuclease in primary cultures [53,54]. Here, we demonstrated that LVV-mediated CRISPR-Cas9 in primary HAECS induced high gene modification activity at the targeted locus that was associated with a decrease of the CFTR protein content together with a strong decrease in the I-172-inhibitable transepithelial CFTR currents. Interestingly, transduced HAECs could be cultured at the air-liquid interface leading to a polarized epithelium, and transduction with the active TSJB1 LVV did not affect the transepithelial resistances. This protocol displays several advantages. The reported high transduction efficiency and high modification frequencies reduce the number of cells from one batch that are not selected which is very important as this is precious material. In addition, the continuous expression of CRISPR-Cas9 components is particularly beneficial to introduce bi-allelic silencing mutations in the greatest number of cells, and was not associated to any cytotoxic effect. Research groups are currently working on the differentiation of induced pluripotent stem (iPS) cells into functional respiratory epithelial cells [55,56]. Modification of iPS cells with our constructs would allow selection and expansion of specific clones with known mutations. Although future research on the phenotype of these cells is mandatory, these results provide a proof of concept that primary HAECs can be targeted for *CFTR* gene inactivation.

Conclusion

We have generated new *CFTR* knockdown airway epithelial cell lines and demonstrated the application of the lentiviral-mediated CRISPR-Cas9 strategy in primary HAEC cultures with isogenic controls. These results represent a first step to introduce CF-specific mutations at a specific locus by co-expressing small oligonucleotides in airway epithelial cells. This approach will allow the manipulation of CFTR expression and/or monitoring of the consequences of CF-causing mutations in cells with their isogenic controls, a condition that is not reached when comparing cultures of non-CF and CF patients.

Conflict of interest

Acknowledgements

Supplementary material

Supplementary figure 1 shows the siRNA sequences designed to target CFTR mRNA and their silencing efficiency.

Supplementary figure 2 shows shRNA and CRISPR-Cas9 DNA constructs in LVV backbones and provides flow cytometric analyses of transduced Calu-3 cells and primary HAECs.

Supplementary figure 3 depicts the protocol for the generation and analysis of pseudo-stratified human airway epithelia.

Supplementary figure 4 shows typical recording of HAEC cultures transduced with TSJB1 LVVs.

References

[1] Deng Y, Wang CC, Choy KW, Du Q, Chen J, Wang Q, et al. Therapeutic potentials of gene silencing by RNA interference: principles, challenges, and new strategies. Gene 2014;538:217–27. doi:10.1016/j.gene.2013.12.019.

[2] Sakuma T, Barry MA, Ikeda Y. Lentiviral vectors: basic to translational. Biochem J 2012;443:603–18. doi:10.1042/BJ20120146.

[3] Johnson LG, Olsen JC, Naldini L, Boucher RC. Pseudotyped human lentiviral vector-mediated gene transfer to airway epithelia in vivo. Gene Ther 2000;7:568–74. doi:10.1038/sj.gt.3301138.

[4] Borok Z, Harboe-Schmidt JE, Brody SL, You Y, Zhou B, Li X, et al. Vesicular stomatitis virus G-pseudotyped lentivirus vectors mediate efficient apical transduction of polarized quiescent primary alveolar epithelial cells. J Virol 2001;75:11747–54. doi:10.1128/JVI.75.23.11747-11754.2001.

[5] Copreni E, Penzo M, Carrabino S, Conese M. Lentivirus-mediated gene transfer to the respiratory epithelium: a promising approach to gene therapy of cystic fibrosis. Gene Ther 2004;11 Suppl 1:S67–75. doi:10.1038/sj.gt.3302372.

[6] Bos TJ, De Bruyne E, Heirman C, Vanderkerken K. In search of the most suitable lentiviral shRNA system. Curr Gene Ther 2009;9:192–211.

[7] Hsu PD, Lander ES, Zhang F. Development and applications of CRISPR-Cas9 for genome engineering. Cell 2014;157:1262–78. doi:10.1016/j.cell.2014.05.010.

[8] Jinek M, Chylinski K, Fonfara I, Hauer M, Doudna JA, Charpentier E. A programmable dual-RNA-guided DNA endonuclease in adaptive bacterial immunity. Science 2012;337:816–21. doi:10.1126/science.1225829.

[9] Malina A, Mills JR, Cencic R, Yan Y, Fraser J, Schippers LM, et al. Repurposing CRISPR/Cas9 for in situ functional assays. Genes Dev 2013;27:2602–14. doi:10.1101/gad.227132.113.

[10] Kaur IP, Chopra K, Rishi P, Puri S, Sharma G. Small RNAs: the qualified candidates for gene manipulation in diverse clinical pathologies. Crit Rev Ther Drug Carrier Syst 2014;31:305–29.

[11] Cai M, Yang Y. Targeted genome editing tools for disease modeling and gene therapy. Curr Gene Ther 2014;14:2–9.

[12] Schwank G, Koo B-K, Sasselli V, Dekkers JF, Heo I, Demircan T, et al. Functional repair of CFTR by CRISPR/Cas9 in intestinal stem cell organoids of cystic fibrosis patients. Cell Stem Cell 2013;13:653–8. doi:10.1016/j.stem.2013.11.002.

[13] Rowe SM, Miller S, Sorscher EJ. Cystic fibrosis. N Engl J Med 2005;352:1992–2001. doi:10.1056/NEJMra043184.

[14] Wilke M, Buijs-Offerman RM, Aarbiou J, Colledge WH, Sheppard DN, Touqui L, et al. Mouse models of cystic fibrosis: phenotypic analysis and research applications. J Cyst Fibros Off J Eur Cyst Fibros Soc 2011;10 Suppl 2:S152–71. doi:10.1016/S1569-1993(11)60020-9.

[15] Rogers CS, Stoltz DA, Meyerholz DK, Ostedgaard LS, Rokhlina T, Taft PJ, et al. Disruption of the CFTR gene produces a model of cystic fibrosis in newborn pigs. Science 2008;321:1837–41. doi:10.1126/science.1163600.

[16] Ostedgaard LS, Meyerholz DK, Chen J-H, Pezzulo AA, Karp PH, Rokhlina T, et al. The ΔF508 mutation causes CFTR misprocessing and cystic fibrosis-like disease in pigs. Sci Transl Med 2011;3:74ra24. doi:10.1126/scitranslmed.3001868.

[17] Stoltz DA, Rokhlina T, Ernst SE, Pezzulo AA, Ostedgaard LS, Karp PH, et al. Intestinal CFTR expression alleviates meconium ileus in cystic fibrosis pigs. J Clin Invest 2013;123:2685–93. doi:10.1172/JCI68867.

[18] Sun X, Sui H, Fisher JT, Yan Z, Liu X, Cho H-J, et al. Disease phenotype of a ferret CFTR-knockout model of cystic fibrosis. J Clin Invest 2010;120:3149–60. doi:10.1172/JCI43052.

[19] Gruenert DC, Willems M, Cassiman JJ, Frizzell RA. Established cell lines used in cystic fibrosis research. J Cyst Fibros Off J Eur Cyst Fibros Soc 2004;3 Suppl 2:191–6. doi:10.1016/j.jcf.2004.05.040.

[20] Shan J, Huang J, Liao J, Robert R, Hanrahan JW. Anion secretion by a model epithelium: more lessons from Calu-3. Acta Physiol Oxf Engl 2011;202:523–31. doi:10.1111/j.1748-1716.2011.02253.x.

[21] Randell SH, Fulcher ML, O'Neal W, Olsen JC. Primary epithelial cell models for cystic fibrosis research. Methods Mol Biol Clifton NJ 2011;742:285–310. doi:10.1007/978-1-61779-120-8_18.

[22] Ramachandran S, Krishnamurthy S, Jacobi AM, Wohlford-Lenane C, Behlke MA, Davidson BL, et al. Efficient delivery of RNA interference oligonucleotides to polarized airway epithelia in vitro. Am J Physiol Lung Cell Mol Physiol 2013;305:L23–32. doi:10.1152/ajplung.00426.2012.

[23] Wiszniewski L, Jornot L, Dudez T, Pagano A, Rochat T, Lacroix JS, et al. Long-term cultures of polarized airway epithelial cells from patients with cystic fibrosis. Am J Respir Cell Mol Biol 2006;34:39–48. doi:10.1165/rcmb.2005-0161OC.

[24]   Nguyen TH, Oberholzer J, Birraux J, Majno P, Morel P, Trono D. Highly efficient lentiviral vector-mediated transduction of nondividing, fully reimplantable primary hepatocytes. Mol Ther J Am Soc Gene Ther 2002;6:199–209.

[25]   Hsu PD, Scott DA, Weinstein JA, Ran FA, Konermann S, Agarwala V, et al. DNA targeting specificity of RNA-guided Cas9 nucleases. Nat Biotechnol 2013;31:827–32. doi:10.1038/nbt.2647.

[26]   Quinton PM. Too much salt, too little soda: cystic fibrosis. Sheng Li Xue Bao 2007;59:397–415.

[27]   Trapani I, Puppo A, Auricchio A. Vector platforms for gene therapy of inherited retinopathies. Prog Retin Eye Res 2014. doi:10.1016/j.preteyeres.2014.08.001.

[28]   Aarbiou J, Copreni E, Buijs-Offerman RM, van der Wegen P, Castellani S, Carbone A, et al. Lentiviral small hairpin RNA delivery reduces apical sodium channel activity in differentiated human airway epithelial cells. J Gene Med 2012;14:733–45. doi:10.1002/jgm.2672.

[29]   Caci E, Melani R, Pedemonte N, Yueksekdag G, Ravazzolo R, Rosenecker J, et al. Epithelial sodium channel inhibition in primary human bronchial epithelia by transfected siRNA. Am J Respir Cell Mol Biol 2009;40:211–6. doi:10.1165/rcmb.2007-0456OC.

[30]   Florea BI, Meaney C, Junginger HE, Borchard G. Transfection efficiency and toxicity of polyethylenimine in differentiated Calu-3 and nondifferentiated COS-1 cell cultures. AAPS PharmSci 2002;4:E12. doi:10.1208/ps040312.

[31]   Forbes B, Ehrhardt C. Human respiratory epithelial cell culture for drug delivery applications. Eur J Pharm Biopharm Off J Arbeitsgemeinschaft Für Pharm Verfahrenstechnik EV 2005;60:193–205. doi:10.1016/j.ejpb.2005.02.010.

[32]   Palmer ML, Lee SY, Maniak PJ, Carlson D, Fahrenkrug SC, O'Grady SM. Protease-activated receptor regulation of Cl- secretion in Calu-3 cells requires prostaglandin release and CFTR activation. Am J Physiol Cell Physiol 2006;290:C1189–98. doi:10.1152/ajpcell.00464.2005.

[33]   MacVinish LJ, Cope G, Ropenga A, Cuthbert AW. Chloride transporting capability of Calu-3 epithelia following persistent knockdown of the cystic fibrosis transmembrane conductance regulator, CFTR. Br J Pharmacol 2007;150:1055–65. doi:10.1038/sj.bjp.0707175.

[34]   Losa D, Köhler T, Bellec J, Dudez T, Crespin S, Bacchetta M, et al. Pseudomonas aeruginosa-induced apoptosis in airway epithelial cells is mediated by gap junctional communication in a JNK-dependent manner. J Immunol Baltim Md 1950 2014;192:4804–12. doi:10.4049/jimmunol.1301294.

[35]   Sesma JI, Kreda SM, Okada SF, van Heusden C, Moussa L, Jones LC, et al. Vesicular nucleotide transporter regulates the nucleotide content in airway epithelial mucin granules. Am J Physiol Cell Physiol 2013;304:C976–84. doi:10.1152/ajpcell.00371.2012.

[36]   Huang J, Shan J, Kim D, Liao J, Evagelidis A, Alper SL, et al. Basolateral chloride loading by the anion exchanger type 2: role in fluid secretion by the human airway epithelial cell line Calu-3. J Physiol 2012;590:5299–316. doi:10.1113/jphysiol.2012.236919.

[37]   Engelman JA, Jänne PA, Mermel C, Pearlberg J, Mukohara T, Fleet C, et al. ErbB-3 mediates phosphoinositide 3-kinase activity in gefitinib-sensitive non-small cell lung cancer cell lines. Proc Natl Acad Sci U S A 2005;102:3788–93. doi:10.1073/pnas.0409773102.

[38]   Grimm D. The dose can make the poison: lessons learned from adverse in vivo toxicities caused by RNAi overexpression. Silence 2011;2:8. doi:10.1186/1758-907X-2-8.

[39]   Börner K, Niopek D, Cotugno G, Kaldenbach M, Pankert T, Willemsen J, et al. Robust RNAi enhancement via human Argonaute-2 overexpression from plasmids, viral vectors and cell lines. Nucleic Acids Res 2013;41:e199. doi:10.1093/nar/gkt836.

[40]   Kälin N, Claass A, Sommer M, Puchelle E, Tümmler B. DeltaF508 CFTR protein expression in tissues from patients with cystic fibrosis. J Clin Invest 1999;103:1379–89. doi:10.1172/JCI5731.

[41]   Penque D, Mendes F, Beck S, Farinha C, Pacheco P, Nogueira P, et al. Cystic fibrosis F508del patients have apically localized CFTR in a reduced number of airway cells. Lab Investig J Tech Methods Pathol 2000;80:857–68.

[42]   Borthwick LA, Botha P, Verdon B, Brodlie MJ, Gardner A, Bourn D, et al. Is CFTR-delF508 really absent from the apical membrane of the airway epithelium? PloS One 2011;6:e23226. doi:10.1371/journal.pone.0023226.

[43]   Derichs N, Mekus F, Bronsveld I, Bijman J, Veeze HJ, von der Hardt H, et al. Cystic fibrosis transmembrane conductance regulator (CFTR)-mediated residual chloride secretion does not protect against early chronic Pseudomonas aeruginosa infection in F508del homozygous cystic fibrosis patients. Pediatr Res 2004;55:69–75. doi:10.1203/01.PDR.0000100758.66805.CE.

[44]   Stanke F, Hedtfeld S, Becker T, Tümmler B. An association study on contrasting cystic fibrosis endophenotypes recognizes KRT8 but not KRT18 as a modifier of cystic fibrosis disease severity and CFTR mediated residual chloride secretion. BMC Med Genet 2011;12:62. doi:10.1186/1471-2350-12-62.

[45]   Stanke F, van Barneveld A, Hedtfeld S, Wölfl S, Becker T, Tümmler B. The CF-modifying gene EHF promotes p.Phe508del-CFTR residual function by altering protein glycosylation and trafficking in epithelial cells. Eur J Hum Genet EJHG 2014;22:660–6. doi:10.1038/ejhg.2013.209.

[46]   Hajj R, Lesimple P, Nawrocki-Raby B, Birembaut P, Puchelle E, Coraux C. Human airway surface epithelial regeneration is delayed and abnormal in cystic fibrosis. J Pathol 2007;211:340–50. doi:10.1002/path.2118.

[47]   Kirk KL. CFTR channels and wound healing. Focus on "Cystic fibrosis transmembrane conductance regulator is involved in airway epithelial wound repair." Am J Physiol Cell Physiol 2010;299:C888–90. doi:10.1152/ajpcell.00313.2010.

[48]   Trinh NTN, Bardou O, Privé A, Maillé E, Adam D, Lingée S, et al. Improvement of defective cystic fibrosis airway epithelial wound repair after CFTR rescue. Eur Respir J 2012;40:1390–400. doi:10.1183/09031936.00221711.

[49]   Tabary O, Zahm JM, Hinnrasky J, Couetil JP, Cornillet P, Guenounou M, et al. Selective up-regulation of chemokine IL-8 expression in cystic fibrosis bronchial gland cells in vivo and in vitro. Am J Pathol 1998;153:921–30. doi:10.1016/S0002-9440(10)65633-7.

[50]   Perez A, Issler AC, Cotton CU, Kelley TJ, Verkman AS, Davis PB. CFTR inhibition mimics the cystic fibrosis inflammatory profile. Am J Physiol Lung Cell Mol Physiol 2007;292:L383–95. doi:10.1152/ajplung.00403.2005.

[51]   Vij N, Mazur S, Zeitlin PL. CFTR is a negative regulator of NFkappaB mediated innate immune response. PloS One 2009;4:e4664. doi:10.1371/journal.pone.0004664.

[52]   Hunter MJ, Treharne KJ, Winter AK, Cassidy DM, Land S, Mehta A. Expression of wild-type CFTR suppresses NF-kappaB-driven inflammatory signalling. PloS One 2010;5:e11598. doi:10.1371/journal.pone.0011598.

[53]   Koike-Yusa H, Li Y, Tan E-P, Velasco-Herrera MDC, Yusa K. Genome-wide recessive genetic screening in mammalian cells with a lentiviral CRISPR-guide RNA library. Nat Biotechnol 2014;32:267–73. doi:10.1038/nbt.2800.

[54]   Kabadi AM, Ousterout DG, Hilton IB, Gersbach CA. Multiplex CRISPR/Cas9-based genome engineering from a single lentiviral vector. Nucleic Acids Res 2014. doi:10.1093/nar/gku749.

[55]   Huang SXL, Islam MN, O'Neill J, Hu Z, Yang Y-G, Chen Y-W, et al. Efficient generation of lung and airway epithelial cells from human pluripotent stem cells. Nat Biotechnol 2014;32:84–91. doi:10.1038/nbt.2754.

[56]   Firth AL, Dargitz CT, Qualls SJ, Menon T, Wright R, Singer O, et al. Generation of multiciliated cells in functional airway epithelia from human induced pluripotent stem cells. Proc Natl Acad Sci U S A 2014;111:E1723–30. doi:10.1073/pnas.1403470111.

Figure 1. CRISPR-Cas9 genome editing activity in transduced Calu-3 cells and primary HAECs. (A) Calu-3 cells were transduced with a dose range of CRISPR-Cas9 LVVs. Multiplicity of infection (MOI) is indicated above the diagram. A week post-transduction (PT), percentage of GFP positive cells (GFP + cells %) was determined by FACS and gDNA was extracted to perform T7E1 mismatch detection assay at the target locus in *CFTR* exon 2. Gene modification activity (GMA) was calculated as described in the Materials and Methods and expressed as a percentage of cleavage normalized to the percentage of GFP positive cells. (B) Frequency of gene modification was monitored during CRISPR-Cas9 Calu-3 cell line expansion on days 25 and 65 PT (D25 PT and D65 PT respectively, n=3). (C) Potential off-target effects were investigated at four loci corresponding to the most probable genome-wide off-target sites for TSJB1 sequence (n=3). The T7E1 mismatch detection assay was performed in CRISPR-Cas9 Calu-3 cells on D65 PT. (D) Primary HAECs (n=2 patients) were transduced with CRISPR-Cas9 LVVs at MOIs 2 and 10. A week PT, GFP positive cells were sorted by FACS and gDNA was extracted from this subpopulation to perform a T7E1 mismatch detection assay at the target locus of *CFTR* exon 2. UTC: untransduced cells, TSJB1 and 2: target sequences JB1 and JB2, OFF-TS1-4: off-target sequences 1-4, *: non-cleaved PCR product, arrow: cleaved PCR product.

Figure 2. Silencing of CFTR mRNA and protein expression by shRNA interference and CRISPR-Cas9 genome editing in polarized Calu-3 cells. shAlter and sh1+sh2 Calu-3 cells (A, C) and CTL and TSJB1 Calu-3 cells (B, D) were seeded on semi-permeable supports and cultured under submerged conditions for 14-20 days alongside non modified Calu-3 cells (UTC). (A, B) Total RNAs were extracted and CFTR mRNA abundance was quantified by RT-qPCR (n=10, 7, 6 for shRNA cell lines and n=7, 8, 8 for CRISPR-Cas9 cell lines). (B, D) Proteins were extracted and processed for Western blot. CFTR protein expression was quantified by densitometry and normalized to GAPDH house-keeping gene expression (n=6, 5, 6 for shRNA cell lines and n=6, 8, 8 for CRISPR-Cas9 cell lines). Bars indicate means ± SEM. Significant difference compared to shAlter or CTL cells (p<0.05) is indicated by one or more asterisks.

Figure 3. Silencing of CFTR-mediated transepithelial currents in polarized Calu-3 cells. shAlter, sh1+sh2, CTL and TSJB1 Calu-3 cells were seeded on semi-permeable supports and cultured under submerged conditions for 14-20 days alongside untransduced Calu-3 cells (UTC). (A) Representative recordings of transepithelial short-circuit currents (Isc) with CRISPR-Cas9-modified Calu-3 cells. Note that fluid currents were not cancelled so that the zero value on the Y-axis does not represent the true zero current level. (B, C) Transepithelial Isc was recorded in Ussing chamber device after stabilization of the monolayers (Isc_{basal}), CFTR activation by isoproterenol ($Isc_{act. CFTR}$) and CFTR inhibition by I-172 ($Isc_{inh. CFTR}$) (n=9, 10, 10 for shRNA Calu-3 cells and n=8, 8, 7 for CRISPR-Cas9 Calu-3 cells). (D, E) Relative fold change of the transepithelial Isc following inhibition by I-172 accounts for *CFTR* knock-down at the electrophysiological level. Bars indicate means ± SEM. Significant difference compared to shAlter or CTL cells (p<0.05) is indicated by one or more asterisks. I: isoproterenol, I-172: CFTR inhibitor I-172.

Figure 4. Silencing of CFTR-mediated transepithelial currents in differentiated primary HAECs by CRISPR-Cas9 genome editing. Primary HAECs were transduced with shRNA and CRISPR-Cas9 LVVs and processed as described in Supplementary figure 2. (A, B) Proteins were extracted and processed for Western blot.

CFTR protein expression was quantified by densitometry and normalized to GAPDH house-keeping gene expression (n=3-6 in A and n=3 in B). (C, D) Transepithelial resistances were measured in Ussing chamber device to confirm primary culture polarization. (E, F) Transepithelial short-circuit current variations in response to CFTR-blocker I-172 were measured in Ussing chamber device following ENaC inhibition by amiloride and CFTR activation by isoproterenol (n=4-5 in E and n=3-7 in F). Bars indicate means ± SEM. Significant difference compared to shAlter, CTL or UTC cells ($p<0.05$) is indicated by one or more asterisks.

Figure 5. CRISPR/shRNA double knock-down in polarized Calu-3 cells. CTL and TSJB1 Calu-3 cells were transduced with shAlter and sh1+sh2 LVVs respectively (MOI 10), expanded and finally cultured on semi-permeable supports under submerged conditions for 14-20 days. (A) CFTR mRNA abundance was measured by RT-qPCR (n=4). (B) Western blot analysis of the CFTR protein content was performed by densitometry and normalization to GAPDH house-keeping gene expression (n=4). (C, D) Transepithelial short-circuit currents (Isc) were measured in Ussing chamber device after stabilization of the monolayers (Isc_{basal}), CFTR activation by isoproterenol ($Isc_{act. CFTR}$) and CFTR inhibition by the I-172 blocker ($Isc_{inh. CFTR}$) (n=5). (E) CFTR inhibition is depicted as a relative fold change of the transepithelial Isc following inhibition by Gly-H101. Bars indicate means ± SEM. Statistical significance compared to CTL/shAlter cells ($p<0.05$) is indicated by one or more asterisks. I: isoproterenol, I-172: CFTR inhibitor I-172.

Figure 6. Characterization of CRISPR-Cas9-modified Calu-3 cells and HAECs. (A) To assess their migration and proliferation profile, CTL and TSJB1 Calu-3 cells were seeded on Ibidi inserts. Gap area was photographed when the inserts were removed (t=0h) and at the end of the experiment (t=15h). Images were merged and pixels in the non-repaired area were counted. Results are indicated as a ratio of pixel numbers (n=10 and 11). (B) At the end of the experiment, cells were stained with the nuclear proliferation marker Ki-67 and DAPI. Pictures were taken in n=5 areas (n=5 inserts for a total of n=25). Results are indicated as a ratio of Ki-67 positive cells/DAPI positive cells. (C, D) Basal IL-8 secretion was measured in apical (C) and basolateral (D) media from CRISPR-Cas9 Calu-3 cells (n=6) by ELISA, normalized to total protein amounts and expressed as a fold change compared to untransduced Calu-3 cells. (E, F) HAECs were allowed to differentiate for 30 days and three inserts of untransduced, (UTC) and transduced with CTL and TSJB1 LVVs were used for IL-8 secretion detection in triplicate. Fold change of total IL-8 secretion is expressed compared to UTC cells. Bars indicate means ± SEM. Statistical significance compared to CTL cells ($p<0.05$) is indicated by one or more asterisks.
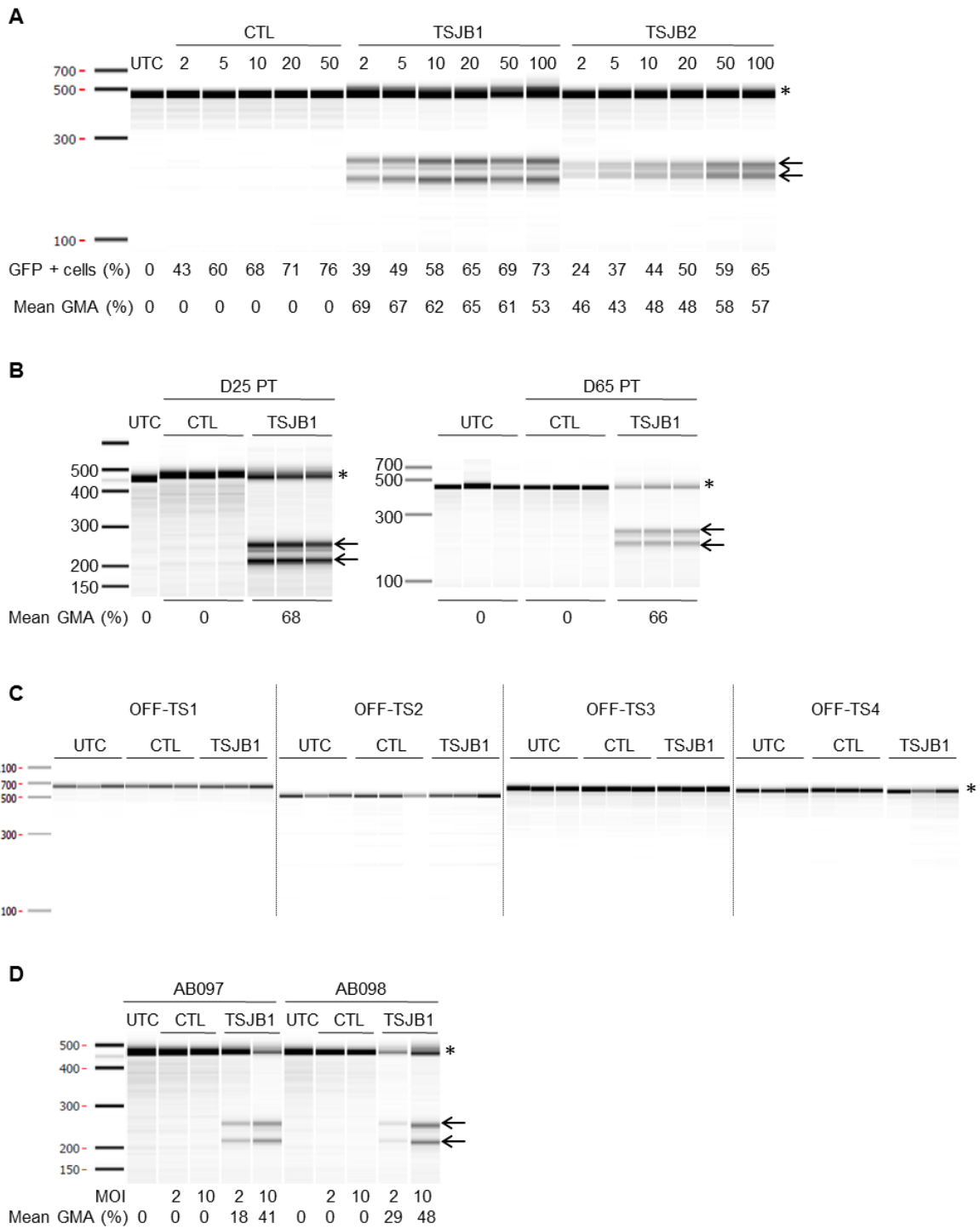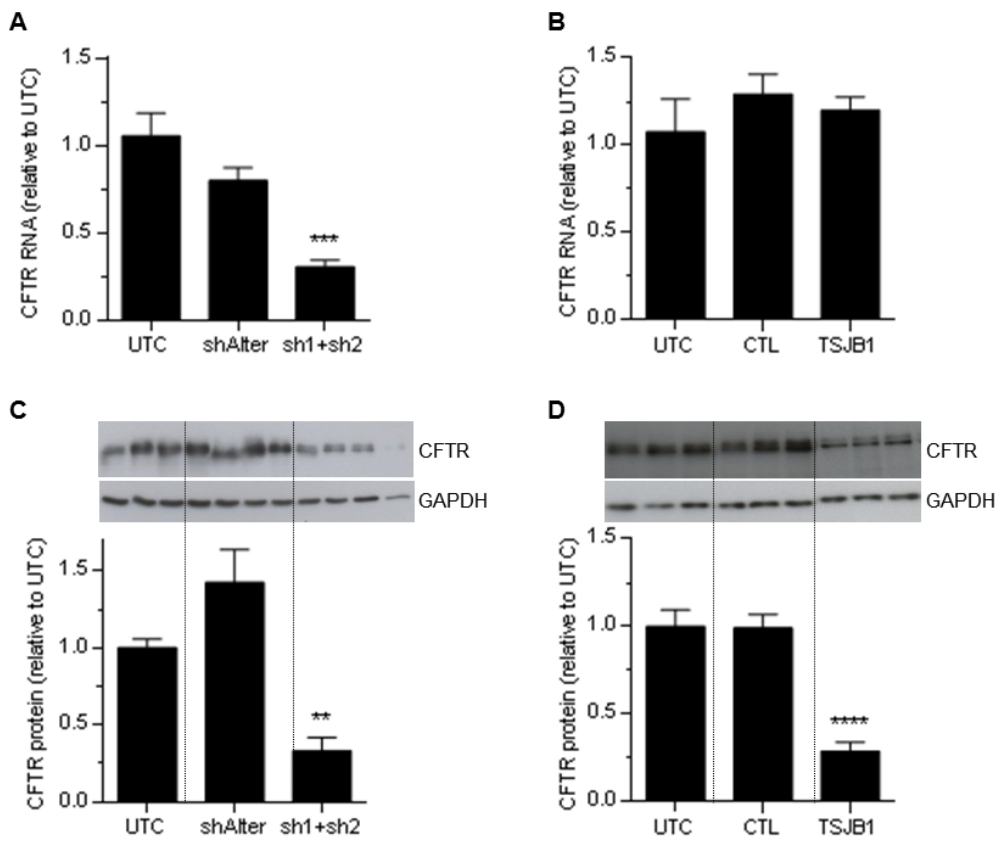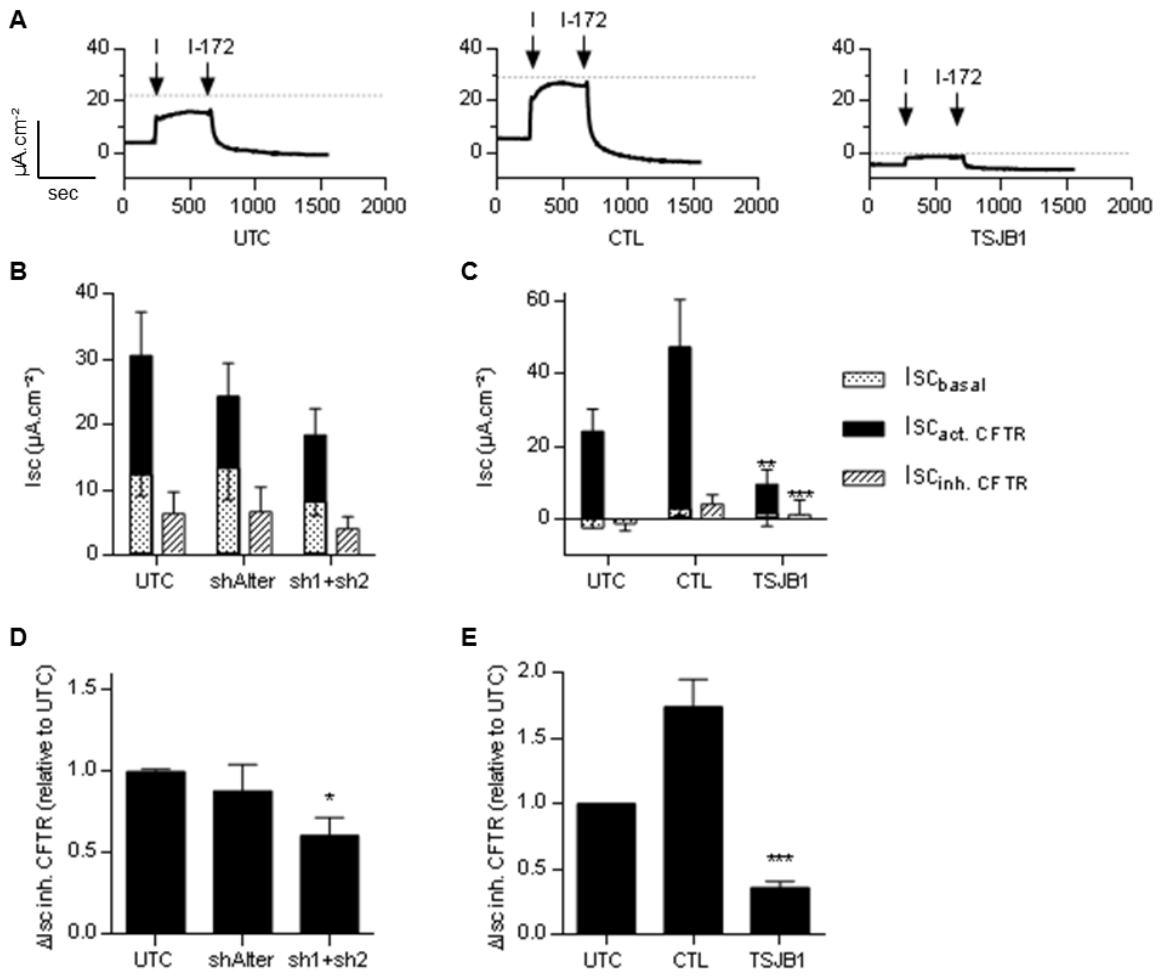
Figure 1

A

	UTC	CTL						TSJB1						TSJB2					
		2	5	10	20	50		2	5	10	20	50	100	2	5	10	20	50	100
GFP + cells (%)	0	43	60	68	71	76		39	49	58	65	69	73	24	37	44	50	59	65
Mean GMA (%)	0	0	0	0	0	0		69	67	62	65	61	53	46	43	48	48	58	57

B

		D25 PT						D65 PT		
	UTC	CTL	TSJB1		UTC		CTL		TSJB1	
Mean GMA (%)	0	0	68		0		0		66	

C

OFF-TS1   OFF-TS2   OFF-TS3   OFF-TS4
UTC CTL TSJB1   UTC CTL TSJB1   UTC CTL TSJB1   UTC CTL TSJB1

D

		AB097				AB098			
	UTC	CTL		TSJB1		UTC	CTL		TSJB1
MOI		2	10	2	10		2	10	2	10
Mean GMA (%)	0	0	0	18	41	0	0	0	29	48

Figure 2

Figure 3

Figure 4

Figure 5
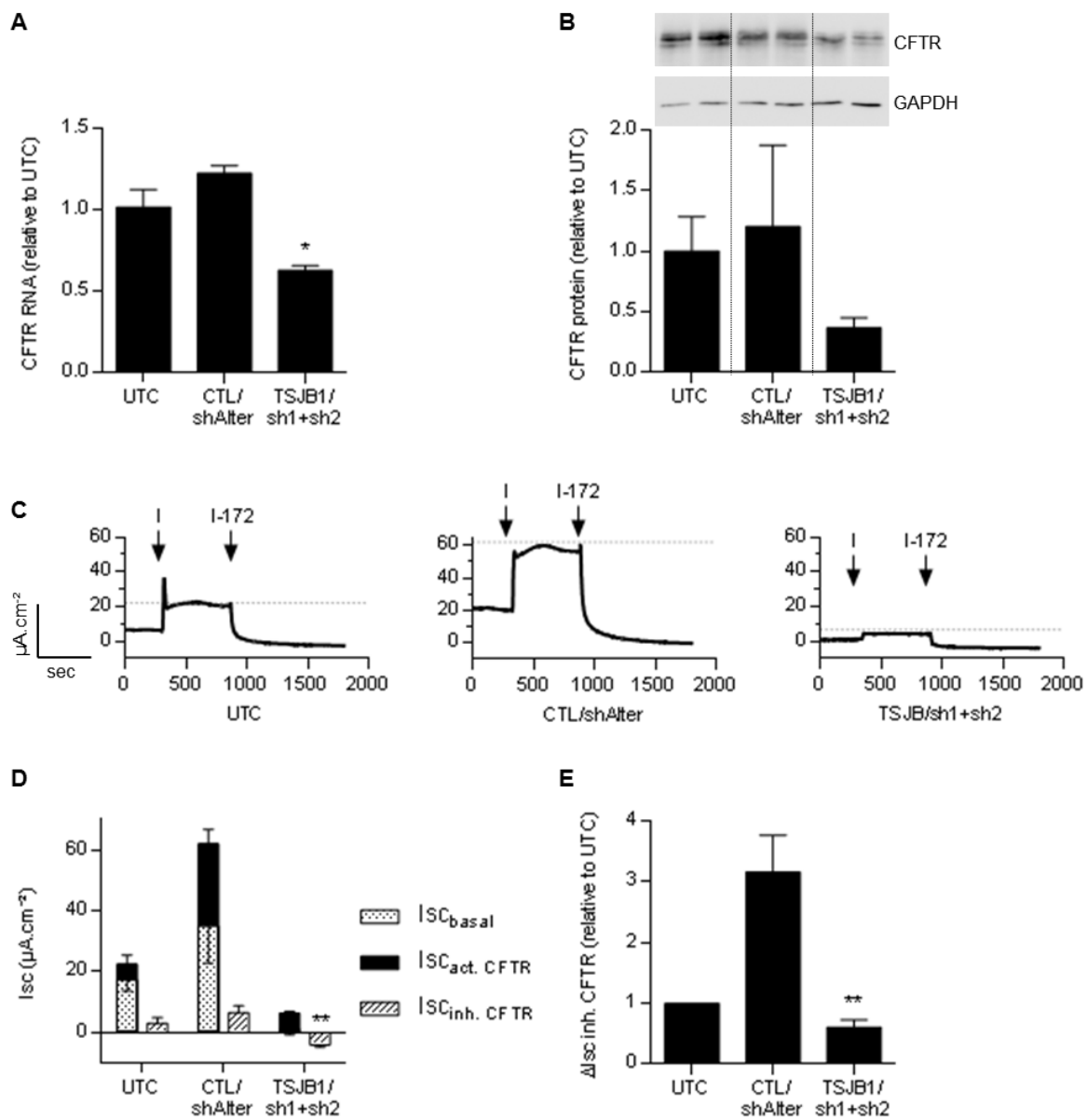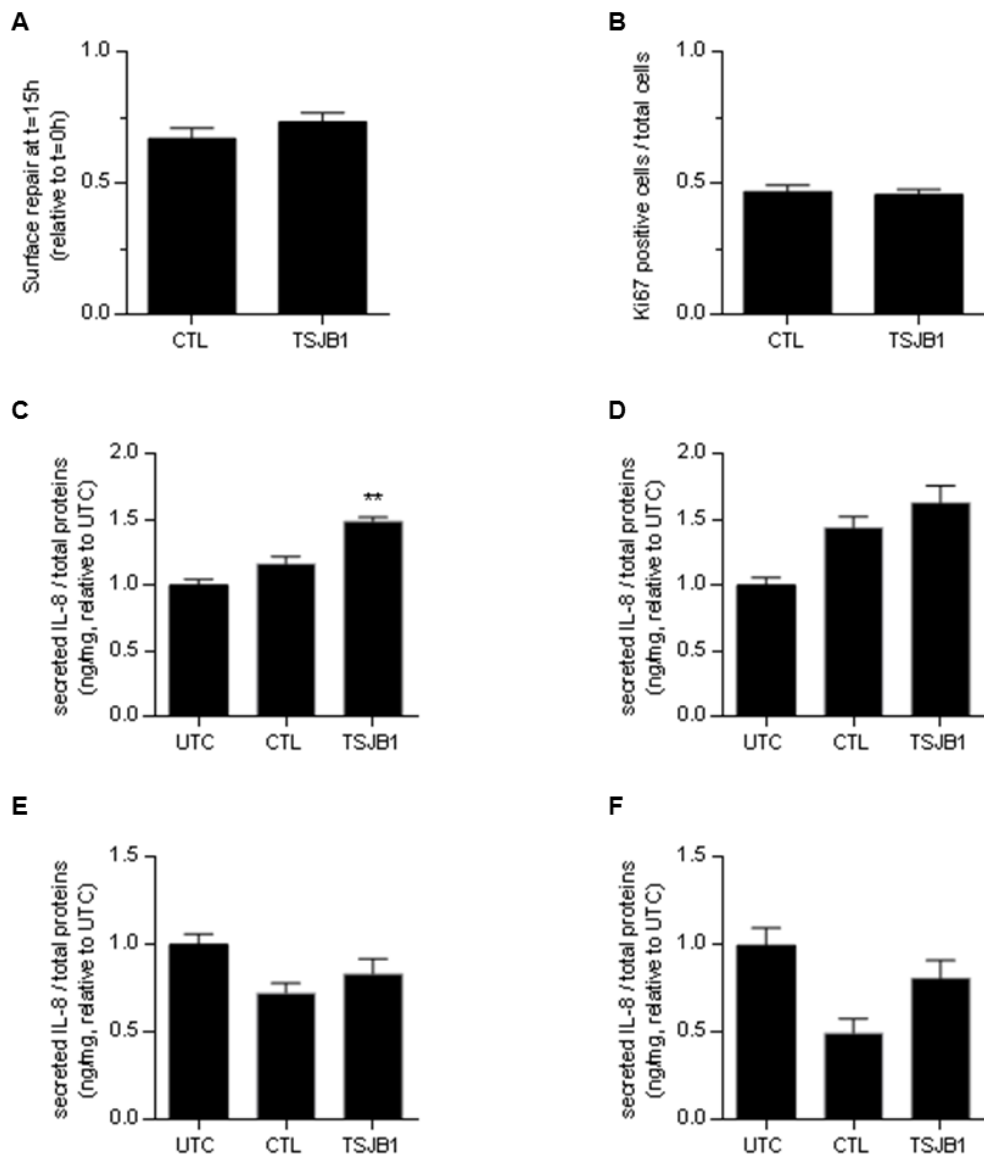
A


B

C

D

E
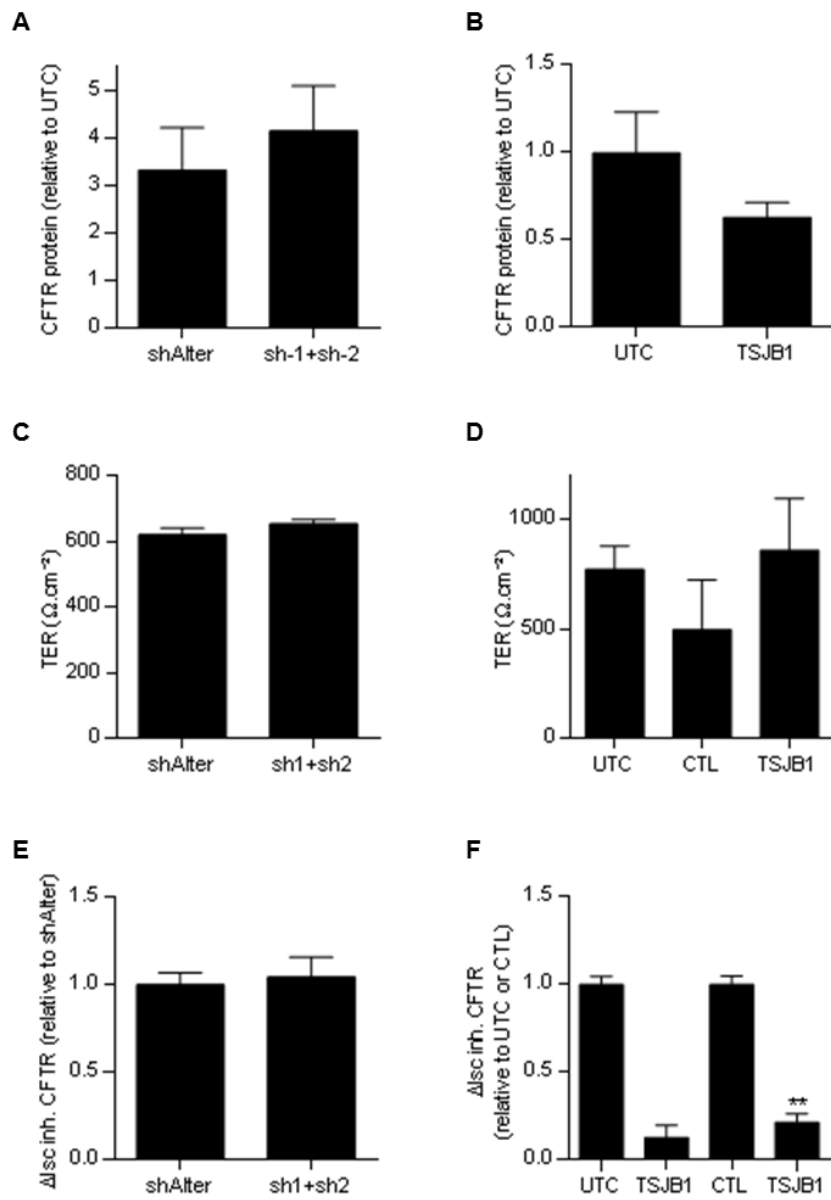
Figure 6

Supplementary figure 1. Screening of siRNA sequences targeting CFTR mRNA. (A) Six siRNA sequences targeting CFTR mRNA were designed using Genelink software and selected for their specificity and the absence of single-nucleotide polymorphisms and insertion/deletion events. Silencing efficiency of these sequences was assessed by transfection of BHK cells expressing CFTR (B) and Calu-3 cells (C). CFTR protein expression was measured by Western blot and quantified by densitometry and normalized to GAPDH house-keeping gene expression. Bars indicate means ± SEM.

A

```
Dav  : GATAGAAAGAGGACAGTTGTTGG
JB19 : CTGGATTATGCCTGGCACCATTA
JB28 : TGATATGGAGAGCATACCAGCAG
JB35 : TTGGATGACCTTCTGCCTCTTAC
JB50 : AACAACAGGAGAAGGAGAAGGAA
JB66 : TCTCTGTGAACACAGGATAGAAG
```
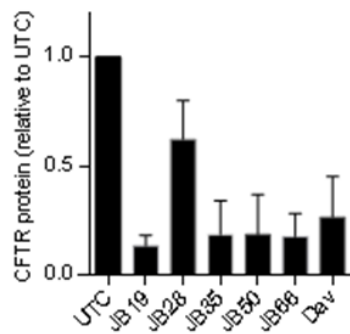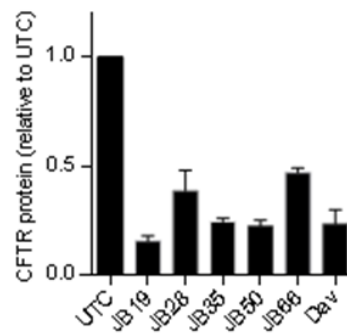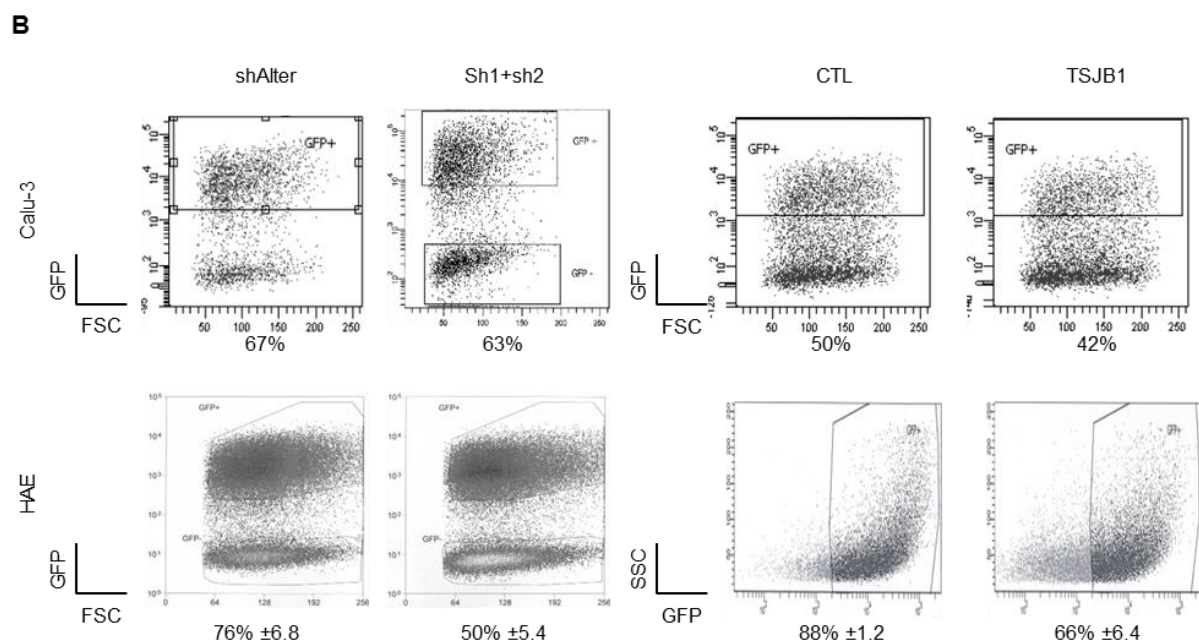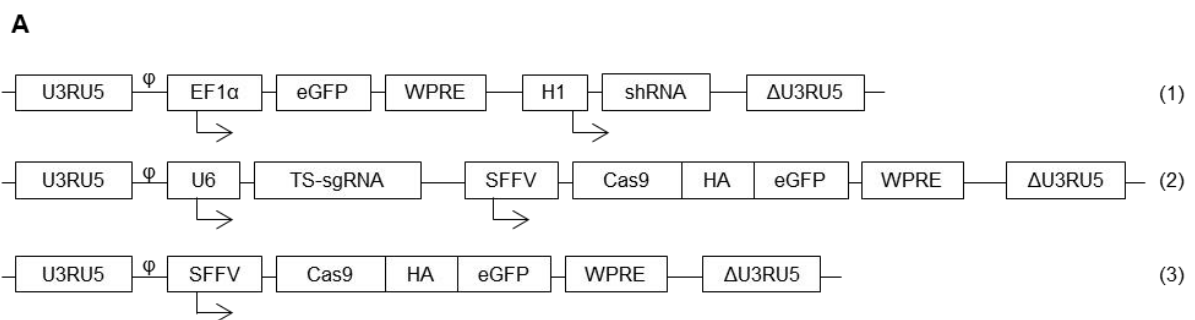
Supplementary figure 2. Generation of *CFTR* knocked-down Calu-3 cell lines and primary human airway epithelial cells (HAECs). (A) DNA constructs in a lentiviral vector (LVV) backbone used to induce *CFTR* gene knock-down. shRNA constructs (1) contain a shRNA sequence targeting CFTR mRNA (sh1, sh2 or sh3) or a non-specific sequence (shAlter) and the eGFP reporter cDNA sequence. CRISPR constructs (2) contain the expression cassette of Cas9 endonuclease fused to HA tag and eGFP cDNA sequence. The 20 nucleotide sequences targeting *CFTR* exon 2 (TS) were cloned upstream the sgRNA sequence. The CRISPR control plasmid (CTL) (3) only expressed the Cas9-HA-eGFP cassette. (B) Flow cytometric analyses of transduced Calu-3 cells and primary HAECs. Calu-3 cells were transduced with shRNA LVVs at MOI 10 and CRISPR LVVs at MOI 2. Numerical values indicate the percentage of GFP positive cells. Primary HAECs were transduced with shRNA and CRISPR LVVs at MOI 10. Numerical values indicate the percentage of GFP positive cells (means ± SEM, n=5-6). EF1α: elongation factor 1 α, SFFV: spleen focus forming virus, eGFP: enhanced green fluorescent protein, shRNA: short hairpin RNA, sgRNA: single-guide RNA, HA: hemagglutinin, WPRE: Woodchuck hepatitis virus post-transcriptional regulatory element, U3RU5: HIV-1-derived self-inactivating long terminal repeat (LTR), ΔU3RU5: HIV-1-derived self-inactivating LTR containing U3 depleted of viral enhancer and promoter, φ: packaging signal.

Supplementary figure 3. Protocol for the generation and analyses of pseudo-stratified human airway epithelia. FACS: flow cytometry and cell sorting, ALI: air-liquid interface.
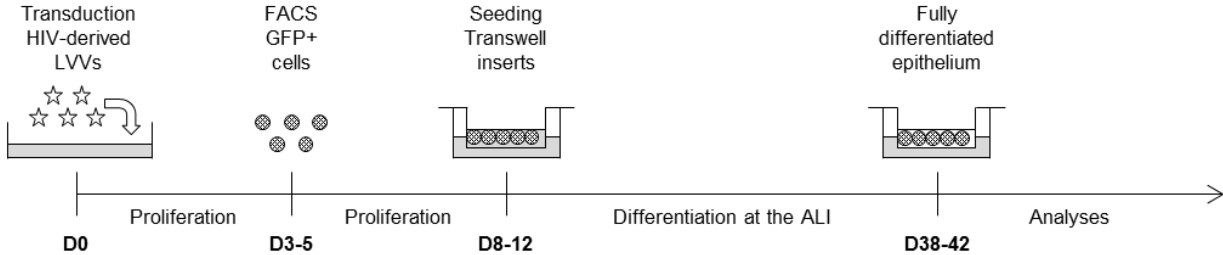
Supplementary figure 4. Silencing of CFTR-mediated transepithelial currents in differentiated primary HAECs by CRISPR-Cas9 genome editing. Representative recordings of transepithelial Iscs in Ussing chamber device after stabilization of the monolayers, inhibition of ENac by amiloride (A), activation of CFTR by isoproterenol (I) and inhibition of CFTR by I-172.